

Phase Diagram of Interacting Bosons on the Honeycomb Lattice

Stefan Wessel

*Institut für Theoretische Physik III, Universität Stuttgart,
Pfaffenwaldring 57, D-70550 Stuttgart, Germany.*

We study the ground state properties of repulsively interacting bosons on the honeycomb lattice using large-scale quantum Monte Carlo simulations. In the hard-core limit the half-filled system develops long ranged diagonal order for sufficiently strong nearest-neighbor repulsion. This staggered solid melts at a first order quantum phase transition into the superfluid phase, without the presence of any intermediate supersolid phase. Within the superfluid phase, both the superfluid density and the compressibility exhibit local minima near particle- (hole-) density one quarter, while the density and the condensate fraction show inflection points in this region. Relaxing the hard-core constraint, supersolid phases emerge for soft-core bosons. The suppression of the superfluid density is found to persist for sufficiently large, finite on-site repulsion.

PACS numbers: 05.30.Jp, 03.75.Lm, 75.10.Jm, 75.40.Mg

The properties of interacting bosons confined to periodic lattice structures are intensively being studied recently. This effort is driven by both the progress in realizing such many-body systems using ultra-cold atoms on optical lattices [1, 2, 3, 4], as well as the interesting phases and quantum phase transitions expected to emerge.

In particular, the ground state can be superfluid, Mott insulating or, in the presence of disorder, a Bose glass [5, 6, 7]. Recently, based on unbiased numerical simulations, also supersolid [8, 9, 10, 11, 12, 13, 14, 15] and exotic valence-bond-solid phases [16] were confirmed to be accessible, and unconventional quantum criticality [14, 16, 17, 18] was discussed for such systems, in particular on non-bipartite, geometrically frustrated two-dimensional lattices, such as the triangular or the Kagome lattice.

Concerning bosons on two-dimensional bipartite, and thus non-frustrated lattices, so far mainly a square lattice structure has also been considered in various other studies [19-31]. However, in light of the recent realization of two-dimensional graphene, with its noticeable properties of fermions on the underlying honeycomb lattice [32, 33, 34, 35], the question arises, how interacting bosons behave on the honeycomb lattice. While both the honeycomb and the square lattice are bipartite, quantum fluctuations are expected to be more relevant on the honeycomb lattice, due to its lowest possible coordination in two dimensions.

Motivated by these considerations, we analyze in this Letter the ground state properties of the extended Bose-Hubbard model

$$H = -t \sum_{\langle i,j \rangle} (b_i^\dagger b_j + b_j^\dagger b_i) + \frac{U}{2} \sum_i n_i(n_i - 1) + V \sum_{\langle i,j \rangle} n_i n_j - \mu \sum_i n_i \quad (1)$$

on the honeycomb lattice. Here, b_i^\dagger (b_i) denote bosonic

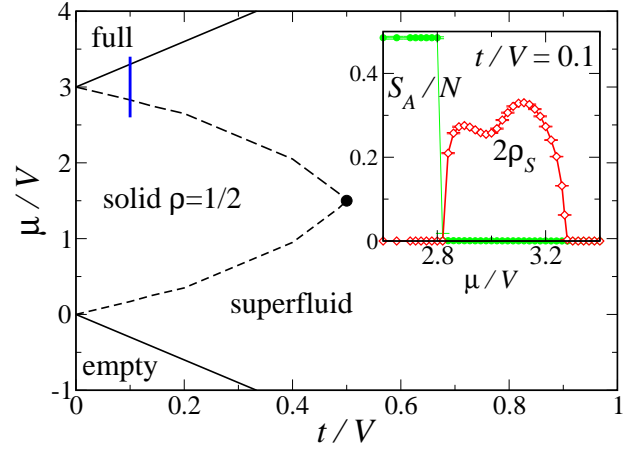


FIG. 1: (Color online) Ground state phase diagram of bosons on the honeycomb lattice in the hard-core limit. The black dot locates the Heisenberg point, where the model has an enhanced $SU(2)$ symmetry. In the inset the superfluid density ρ_s and the structure factor S_A are shown along $t/V = 0.1$ (indicated by the vertical bar in the main part of the figure).

creation (annihilation) operators for bosons on lattice site i , t is the nearest-neighbor hopping amplitude, U an onsite repulsion, V a nearest-neighbor repulsion, and μ the chemical potential in the grand-canonical ensemble, which controls the filling of the lattice.

The honeycomb lattice is bipartite, with a two-site unit cell and a uniform coordination number $z = 3$; the unit cell contains one site from each sublattice. In the following, we employ the stochastic series expansion [36] quantum Monte Carlo (QMC) method with directed loop updates [37, 38], and study the Hamiltonian in Eq. (1) on finite lattices with $N = 2L^2$ sites for L up to 32, at temperatures sufficiently low in order to resolve ground state properties of these finite systems [8]. In contrast to geometrically frustrated lattices, the sign of t in Eq. (1) is irrelevant on the bipartite honeycomb lattice, in that also $t < 0$ would cause no QMC sign problem.

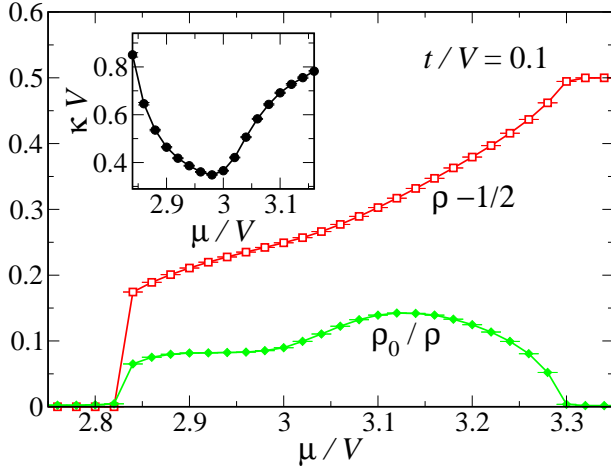


FIG. 2: (Color online) Density ρ (with respect to half-filling) and condensate fraction ρ_0/ρ at $t/V = 0.1$ as functions of μ/V for bosons on the honeycomb lattice in the hard-core limit. The inset shows the compressibility κ which exhibits a local minimum in the superfluid regime.

We first consider the hard-core limit, $U/t \rightarrow \infty$, of Eq. (1), for which the bosonic model can be mapped onto the spin-1/2 XXZ model [39]. This allows for an interpretation of our results in terms of both bosons and quantum spins. The ground state phase diagram of the grand-canonical ensemble in the hard-core limit is shown in Fig. 1. Considering the one-particle and one-hole problem, one finds that for $\mu < -zt$ the system is empty, and for $\mu/V > z(1 + t/V)$ it is fully occupied by one boson per lattice site (density $\rho = 1$). At large values of $t/V > 0.5$, the bosons form a superfluid (SF) with off-diagonal long-range order (ODLRO), characterized by a finite superfluid density, which in the QMC simulations is obtained as $\rho_s = \langle W^2 \rangle / (2\beta t)$ from the particle winding number fluctuations $\langle W^2 \rangle$, where β denotes the inverse temperature [40]. Furthermore, for sufficiently small values of t/V , the system exhibits a solid phase of density $\rho = 1/2$. Its largest extent is set by the Heisenberg point $(t/V, \mu/V) = (1/2, 3/2)$, where the Hamiltonian in Eq. (1) has an enhanced $SU(2)$ symmetry. In the perfect $\rho = 1/2$ solid at $t = 0$, one out of the two sublattices on the honeycomb lattice is occupied, the other being empty (so that reflection symmetry, but not lattice translational symmetry is broken). The corresponding structure factor for this alternating (staggered) diagonal long-range order (DLRO) is thus given by

$$S_A = \frac{1}{N} \sum_{i,j} \epsilon_i \epsilon_j \langle n_i n_j \rangle, \quad (2)$$

where $\epsilon_i = \pm 1$ for i on sublattice $A(B)$, in terms of the density-density correlations. The inset of Fig. 1 shows the evolution of both ρ_s and the order parameter S_A/N along a cut through the phase diagram at $t/V = 0.1$ (the vertical bar in the main part of Fig. 1), and corresponds

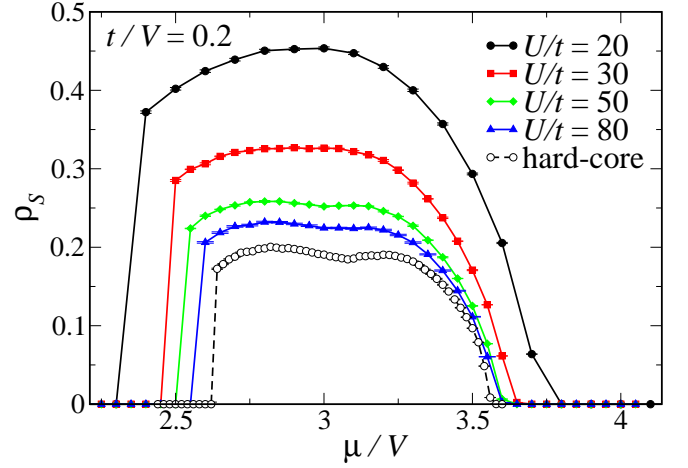


FIG. 3: (Color online) Superfluid density of bosons on the honeycomb lattice at $t/V = 0.2$ as functions of μ/V for various values of U/t , and in the hard-core limit.

to their thermodynamic limit behavior. Both quantities clearly exhibit the first-order nature of the solid-SF quantum phase transition, and the absence of any intermediate supersolid (SS) phase with simultaneous DLRO and ODLRO (only at the Heisenberg point may DLRO and ODLRO co-exist, due to the $SU(2)$ symmetry). In the hard-core limit, the phase diagram of Eq. (1) is thus similar to the one of hard-core bosons on the square lattice [8], irrespectively a rescaled μ -axis, due to the different coordination number ($z = 4$ on the square lattice). In both cases, domain wall proliferation at the quantum melting transition of the half-filled solid renders a SS unstable towards phase separation in the hard-core limit of Eq. (1) [8]. Note, that also through the Heisenberg point the quantum melting of the $\rho = 1/2$ solid is discontinuous [29, 31, 41], despite attempts to extract critical behavior from finite size scaling plots of ρ_s [29, 42]. In fact, the extracted effective dynamical critical exponent z decreases to zero, taking sufficiently large system sizes [41], consistent with the trend observed by comparing the values obtained thus far [29, 42].

In contrast to the case of the square lattice, we observe on the honeycomb lattice a pronounced dip of ρ_s inside the SF phase (c.f. the inset of Fig. 1), with a local minimum at a filling ρ_D close to $3/4$, corresponding to a hole density of $1/4$ ($\rho_D \approx 0.744$ at $(\mu/V)_D \approx 2.97$ for $t/V = 0.1$). Due to particle-hole symmetry in the hard-core limit, this suppression of ρ_s also appears near a particle filling of $\rho = 1/4$. Fig. 3 shows a similar dip in ρ_s for $t/V = 0.2$, where we again find ρ_D close to $3/4$. This indicates the presence of geometric hindrance in the superfluid flow on the honeycomb lattice, well inside the SF region. Indeed, also the compressibility $\kappa = \partial\rho/\partial\mu$ exhibits a minimum at $(\mu/V)_D$, c.f. the inset of Fig. 2. In contrast, as seen in Fig. 2, both

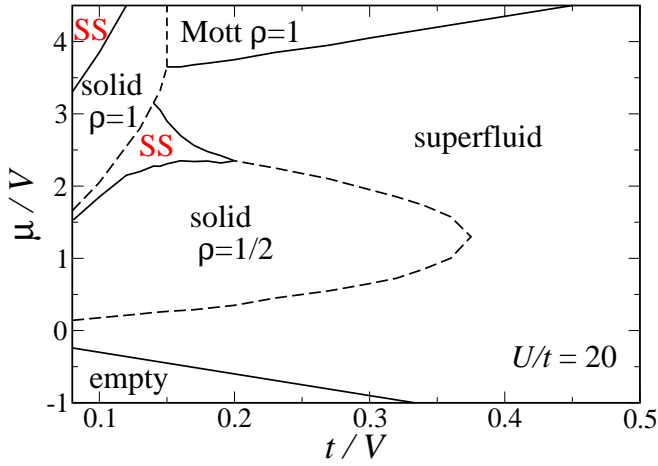


FIG. 4: (Color online) Ground state phase diagram of bosons on the honeycomb lattice for finite $U/t = 20$, with supersolid (SS) phases emerging upon doping the solid phases. Solid (dashed) lines denote continuous (first-order) quantum phase transitions.

the density ρ and the condensate fraction, ρ_0/ρ , where $\rho_0 = \langle b^\dagger(\mathbf{k}=0)b(\mathbf{k}=0) \rangle$, increase in that region upon increasing μ , and show an inflection point at $(\mu/V)_D$. We verified that near the dip the system does *not* exhibit any incommensurate long-range order neither in the density-density nor in bond-bond correlation functions [16].

Extending the analysis beyond the hard-core limit, we next consider soft-core bosons on the honeycomb lattice, and assess the presence of SS phases in this model. Fig. 4 shows the ground state phase diagram for $U/t = 20$ inside the regime where $\rho \leq 1$. The phase diagram exhibits several additional phases; in particular, a SS phase emerges upon doping the $\rho = 1/2$ solid with additional bosons. The simultaneous presence of DLRO and ODLRO within the SS regime for $t/V = 0.14$ and $t/V = 0.16$ can be seen from Fig. 5, by finite values of both S_A/N and ρ_s inside a range of μ/V values. For $(zV - U) \sim t$, the additional particles form a superfluid atop the $\rho = 1/2$ solid background, due to a kinetic energy gain which prevents the domain wall proliferation [8]. Hole doping of the $\rho = 1/2$ solid however does not result in a similar kinetic energy gain, and thus no SS state emerges for $\rho < 1/2$.

The nature of the incompressible state with $\rho = 1$ depends on the ratio zV/U [8]: In the soft-core case, taking $U/t = 20$, we find for $t/V < 0.15$ (i.e., $zV/U > 1$), that the system forms a $\rho = 1$ solid with a finite value of S_A/N in the thermodynamic limit. This $\rho = 1$ solid corresponds to each site of one out of the two sublattices being occupied by two bosons, the other sublattice being empty. In contrast, for $t/V > 0.15$ (i.e., $zV/U < 1$), the system is a uniform $\rho = 1$ Mott insulator, with $S_A/N = 0$. This different behavior at $\rho = 1$ is seen for $t/V = 0.14$

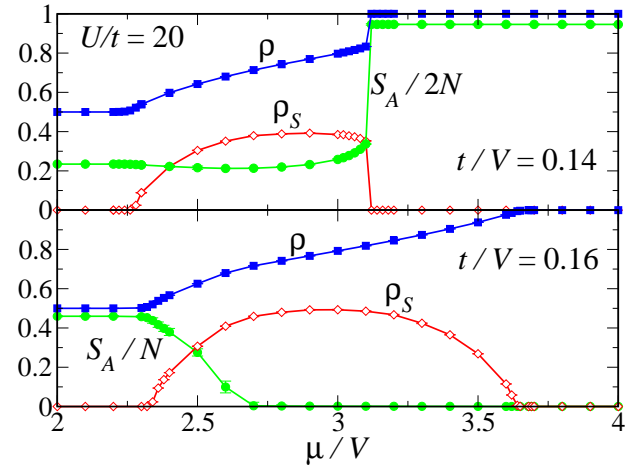


FIG. 5: (Color online) Density ρ , superfluid density ρ_s , and structure factor S_A as functions of μ/V for bosons on the honeycomb lattice for $U/t = 20$ along $t/V = 0.14$ (upper panel) and $t/V = 0.16$ (lower panel).

and $t/V = 0.16$ in Fig. 5, and results from the competition between onsite- and nearest-neighbor repulsion terms in Eq. (1) [8]. Fig. 5 furthermore indicates, that the transition from the $\rho < 1$ SS to the $\rho = 1$ solid is strongly first-order, whereas the SS-SF transition and the SF-Mott transition are continuous, as expected also from kinetic energy considerations [8]. As indicated in Fig. 4, a further SS phase, with $\rho > 1$, emerges out of the $\rho = 1$ solid phase upon further increasing μ . Details of the phase diagram for fillings $\rho > 1$ will be presented elsewhere [43].

For $U/t = 20$, the superfluid density curves in Fig. 5 do not exhibit local minima such as the pronounced dip in ρ_s observed in the hard-core limit (in the inset of Fig. 1). In order to assess, whether this suppression is restricted to the hard-core limit of Eq. (1), we performed simulations also for increasing values of $U/t = 30, 50$, and 80 . In Fig. 3, the resulting values of ρ_s are shown as functions of μ/V for a common value of $t/V = 0.2$, and compared to the hard-core limit. We find that for $U/t = 30$ the superfluid density is almost flat near $\mu/V \approx 2.9$, and for sufficiently large onsite repulsion U , it indeed develops a shallow local minimum, similar to the dip in the hard-core limit. The reduced superfluidity thus relates to the interplay of a large energy penalty for double occupation, and the low connectivity on the honeycomb lattice, compared to the square lattice. In fact, we find that on (inhomogeneous) two-dimensional lattices with an even lower average coordination number $\bar{z} < 3$, the superfluid density gets reduced to zero, and incompressible phases with fractional fillings $\rho = 1/4$ and $3/4$ emerge [43].

In conclusion, we studied the ground state properties of bosons on the honeycomb lattice, as described by

the extended Bose-Hubbard model. We found that the phases and the structure of the phase diagram correspond to those of the same model on the square lattice, both in the hard-core limit and for finite on-site repulsion U . This is anticipated given the bipartiteness of both lattice structures. In particular, a staggered solid phase exists at half-filling for sufficiently strong nearest-neighbor repulsion V . Doping this solid with additional bosons leads to a supersolid phase only for finite values of U , whereas in the hard-core limit and for hole-doping the system phase separates. The incompressible state at filling one is a Mott insulator for dominant $U > zV$, and a staggered solid for $U < zV$. Furthermore, we found that for sufficiently large values of U , both the superfluid density and the compressibility are suppressed inside the superfluid phase at particle fillings of about one quarter and three quarters. As the condensate density does not show a similar reduction, bosons on the honeycomb lattice thus feature regions, where an *increase* of the condensate in the bosonic system contrasts to a *decrease* in its superfluid response.

We would like to thank F. Alet, R. Moessner, and A. Muramatsu for helpful discussions, and NIC Jülich and HRLS Stuttgart for allocation of CPU time.

Note added.- After finishing the numerical calculations, we became aware of a parallel work [42], where results partially similar to our findings are presented.

-
- [1] J. Jaksch *et al.*, Phys. Rev. Lett. **81**, 3108 (1998).
 - [2] M. Greiner *et al.*, Nature **415**, 39 (2002).
 - [3] T. Stöferle, *et al.*, Phys. Rev. Lett. **91**, 130403 (2004).
 - [4] S. Fölling, *et al.*, Phys. Rev. Lett. **97**, 060403 (2006).
 - [5] M. P. A. Fisher, *et al.*, Phys. Rev. B **40**, 546 (1989).
 - [6] R. Scalettar, G. G. Batrouni, and G. T. Zimanyi, Phys. Rev. Lett. **66**, 3144 (1991).
 - [7] J. K. Freericks and H. Monien, Phys. Rev. B **53**, 2691 (1996).
 - [8] P. Sengupta *et al.*, Phys. Rev. Lett. **94**, 207202 (2005).
 - [9] S. Wessel and M. Troyer, Phys. Rev. Lett. **95**, 127205 (2005).
 - [10] R. Melko *et al.*, Phys. Rev. Lett. **95**, 127207 (2005).
 - [11] D. Heidarian and K. Damle, Phys. Rev. Lett. **95**, 127206 (2005).
 - [12] M. Boninsegni and N. Prokof'ev, Phys. Rev. Lett. **95**, 237204 (2005).
 - [13] Jing Yu Gan, Yu Chuan Wen, and Yue Yu, Report cond-mat/0609492.
 - [14] R. G. Melko, A. Del Maestro, and A. A. Burkov, Phys. Rev. B **74**, 214517 (2006).
 - [15] G. G. Batrouni, F. Hebert, and R. T. Scalettar, Phys. Rev. Lett. **97**, 087209 (2006).
 - [16] S. V. Isakov, *et al.*, Phys. Rev. Lett. **97**, 147202 (2006).
 - [17] A. A. Burkov, and L. Balents, Phys. Rev. B **72**, 134502 (2005).
 - [18] K. Sengupta, S. V. Isakov, and Yong Baek Kim, Phys. Rev. B **73**, 245103 (2006).
 - [19] E. Roddick and D. Stroud, Phys. Rev. B **48**, 16600 (1993); *ibid.* **51**, R8672 (1995).
 - [20] A. van Otterlo and K.-H. Wagenblast, Phys. Rev. Lett. **72**, 3598 (1994).
 - [21] A. van Otterlo *et al.*, Phys. Rev. B **52**, 16176 (1995).
 - [22] R. Micnas, S. Robaszkiewicz, and T. Kostyrko, Phys. Rev. B **52**, 6863 (1995).
 - [23] G. G. Batrouni *et al.*, Phys. Rev. Lett. **74**, 2527 (1995).
 - [24] R. T. Scalettar *et al.*, Phys. Rev. B **51**, 8467 (1995).
 - [25] E. S. Sorensen and E. Roddick, Phys. Rev. B **53**, R8867 (1996).
 - [26] E. Frey and L. Balents, Phys. Rev. B **55**, 1050 (1997).
 - [27] M. Kohno and M. Takahashi, Phys. Rev. B **56**, 3212 (1997).
 - [28] G. G. Batrouni, and R. T. Scalettar, Phys. Rev. Lett. **84**, 1599 (2000).
 - [29] F. Hébert *et al.*, Phys. Rev. B **65**, 014513 (2001).
 - [30] G. Schmid *et al.*, Phys. Rev. Lett. **88**, 167208 (2002).
 - [31] A. Kuklov, N. Prokof'ev, and B. Svistunov, Phys. Rev. Lett. **93**, 230402 (2004).
 - [32] Novoselov, K. S. *et al.*, Proc. Natl Acad. Sci. USA **102**, 10451 (2005).
 - [33] Novoselov, K. S. *et al.*, Science **306**, 666 (2004).
 - [34] K.S. Novoselov, *et al.*, Nature **438**, 197 (2005).
 - [35] Y. Zhang, *et al.*, Nature **438**, 201 (2005).
 - [36] A.W. Sandvik, Phys. Rev. B **59**, R14157 (1999).
 - [37] O. F. Syljuåsen and A. W. Sandvik, Phys. Rev. E **66**, 046701 (2002).
 - [38] F. Alet, S. Wessel, and M. Troyer, Phys. Rev. E **71**, 036706 (2005).
 - [39] T. Matsubara and H. Matsuda, Prog. Theor. Phys. **16**, 569 (1956); *ibid.* **17**, 19 (1957).
 - [40] E. L. Pollock and C.M. Ceperley, Phys. Rev. B **36**, 8343 (1987).
 - [41] A. W. Sandvik, and R. Melko, Report cond-mat/0604451.
 - [42] Jin Yu Gan, *et al.*, Report cond-mat/0701120.
 - [43] S. Wessel, in preparation.